

Article

# Dynamic Analysis and DSP Implementation of Memristor Chaotic Systems with Multiple Forms of Hidden Attractors

Zhenggang Guo <sup>1,\*</sup> , Junjie Wen <sup>2</sup> and Jun Mou <sup>2</sup> <sup>1</sup> School of Mechanical Engineering, Dalian University of Technology, Dalian 116023, China<sup>2</sup> School of Mechanical Engineering and Automation, Dalian Polytechnic University, Dalian 116034, China

\* Correspondence: gzg@dlut.edu.cn

**Abstract:** In this paper, a new six dimensional memristor chaotic system is designed by combining the chaotic system with a memristor. By analyzing the phase diagram of the chaotic attractors, eleven different attractors are found, including a multi-wing attractor and symmetric attractors. By analyzing the equilibrium point of the system, it is proven that the system has the property of a hidden chaotic attractor. The dynamic behavior of the system when the three parameters change is analyzed by means of LEs and a Bifurcation diagram. Other phenomenon, such as chaos degradation, coexistence of multiple attractors and bias boosting, are also found. Finally, the simulation on the DSP platform also verifies the accuracy of the chaotic system simulation. The theoretical analysis and simulation results show that the system has rich dynamical characteristics; therefore, it is suitable for secure communication and image encryption and other fields.

**Keywords:** hidden attractor; coexistence of multiple attractors; chaos degradation; offset boosting; DSP

MSC: 34H10



**Citation:** Guo, Z.; Wen, J.; Mou, J. Dynamic Analysis and DSP Implementation of Memristor Chaotic Systems with Multiple Forms of Hidden Attractors. *Mathematics* **2023**, *11*, 24. <https://doi.org/10.3390/math11010024>

Academic Editors: Chunhua Wang and Hairong Lin

Received: 7 December 2022

Revised: 19 December 2022

Accepted: 19 December 2022

Published: 21 December 2022



**Copyright:** © 2022 by the authors. Licensee MDPI, Basel, Switzerland. This article is an open access article distributed under the terms and conditions of the Creative Commons Attribution (CC BY) license (<https://creativecommons.org/licenses/by/4.0/>).

## 1. Introduction

In the 1960s, the proposal of the Lorenz system attracted extensive attention in chaos research. Chaos is a physical phenomenon highly sensitive to initial value. Its development and the related research have made great progress in just a few decades, meanwhile, the study of the chaotic system [1–11] has gradually expanded to weather, finance, communication and other fields. Due to the study of the chaotic system model, many different types of chaotic systems have been derived, such as the discrete chaotic system [12–14], the memristor chaotic system, the hyperchaotic system [15–18] and so on.

The emergence of the memristor [19–22] is also a milestone event for chaos research. Professor Chua predicted the existence of the memristor based on the principle of circuit symmetry in 1971 and sorted out the types and principles of the memristor in subsequent years. In 2008, the HP company successfully developed a memristor to test Chua's theory. At this point, the study of chaos theory entered a new stage, and people began to conjecture and experiment on the connection between the memristor and chaos, which has also become a research hotspot.

A special class of nonlinear dynamical systems with no equilibrium state or infinite equilibrium state can exhibit hidden chaotic attractors [23–26]. In 2013, Leonov and Kuznetsov first proposed a strict mathematical definition of the hidden chaotic attractor. The hidden attractor has the characteristics of possessing a small attractor basin and does not intersect with any unstable equilibrium neighborhood. Due to its hidden characteristics, it has a broad application potential in chaos related fields. In 2008, Professor Chua replaced the Chua diode in Chua's circuit with a piecewise linear memristor; they first proposed the chaotic circuit based on the memristor [27]. In 2010, a chaotic oscillator based on the memcapacitor was presented by Hu [28]. In 2017, Wang designed a chaotic oscillator based

on the meminductor and memcapacitor [29]. In 2019, Yuan designed a simple chaotic oscillator through a memristor, memcapacitor and meminductor in parallel [30].

In this paper, a new memristor chaotic system is constructed based on the memristor and chaotic system. Interestingly, after the stability analysis of the system, the system has a non-equilibrium state, which belongs to the category of chaotic systems with hidden attractors. At the same time, in the process of parameter mediation, it is found that it has many different types of chaotic attractors, which has been relatively rare in the past. In addition, the system also has a variety of complex dynamic phenomena, including a multi-wing chaotic attractor [31–33], symmetric chaotic attractor [34–36], chaotic degradation, coexisting attractor and so on. Offset boosting [37–39] is also a feature of the system, which means that the system can be controlled flexibly through the introduction of feedback states. Finally, the feasibility of the system is verified by the DSP platform. The establishment of the system also provides a new idea for image encryption and secure communication in the future.

The structure of the paper is distributed as follows. In Section 2, the model of the memristor and the chaotic system equation of the memristor are introduced, and the equilibrium point of the system equation is analyzed. In Section 3, the phase diagram of the hidden attractor is presented, and the changes in the LEs and bifurcation diagram corresponding to three different parameters are systematically analyzed. At the same time, the special phenomena of the system are presented, such as chaos degradation, the coexistence of multiple attractors, offset boosting, and complexity analysis. In Section 4, the digital circuit of the system is implemented on the DSP platform, and the correctness of the simulation of the system is verified. Finally, some conclusions are given in Section 5.

## 2. Mathematical Model

The memristor model is shown below.

$$\begin{cases} W(v) = \frac{dq(v)}{d(v)} = \tanh(v) \\ i = W(v)y = \tanh(v)y \\ \frac{d(v)}{dt} = y^2 - v \end{cases} \quad (1)$$

For the sake of showing the characteristic curve of the memristor in more detail, a sinusoidal AC signal  $v = A\sin(2\pi ft)$  is added as the input to the memristor. Let the amplitude  $A = 3$ . As shown in Figure 1, it can be observed that the trajectory of the  $u$ - $i$  feature is similar to an inclined “8”, and the sidelobe area of its characteristic curve will decrease with the increase in frequency, which is consistent with the definition of the memristor.

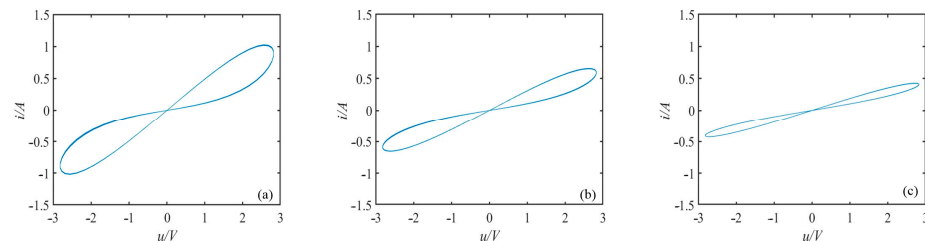


**Figure 1.** The  $u$ - $i$  curve of memristor: (a)  $f = 0.5$  kHz; (b)  $f = 1$  kHz; (c)  $f = 2$  kHz.

### Equilibrium Points Set and Stability

We combined the memristor with the chaotic system to construct a new type of six dimensional chaotic system, and the model of the five dimensional chaotic system we used is as follows:

$$\begin{cases} \dot{x} = -ax + yz + bw + u \\ \dot{y} = cy - xz + k \\ \dot{z} = xy - dz \\ \dot{w} = xz - ew \\ \dot{u} = gy \end{cases} \tag{2}$$

A new 6-D chaotic dynamical system with complex dynamical characteristics is constructed by combining the memristor and chaotic system. The specific formula is as follows:

$$\begin{cases} \dot{x} = -ax + yz + bw + \cos u \\ \dot{y} = cy \tanh v - xz + k \\ \dot{z} = xy - dz \\ \dot{w} = xz - ew \\ \dot{u} = gy \\ \dot{v} = y^2 - v \end{cases} \tag{3}$$

In order to obtain the divergence of the chaotic system (3), the following formulas are listed.

$$\nabla V = \frac{\partial \dot{x}}{\partial x} + \frac{\partial \dot{y}}{\partial y} + \frac{\partial \dot{z}}{\partial z} + \frac{\partial \dot{w}}{\partial w} + \frac{\partial \dot{u}}{\partial u} + \frac{\partial \dot{v}}{\partial v} \tag{4}$$

When the initial conditions of the system are (1, 1, 1, 1, 1, 1) and the parameters are  $a = 3, b = 0.01, c = 7, d = 31, k = 7, e = 5, g = 0.05, l = 6$ , it is easy to establish that the  $\nabla V$  is less than zero, indicating that the system is dissipative, which is also one of the theoretical evidences of the existence of chaos in the system.

Then, when  $\dot{x} = \dot{y} = \dot{z} = \dot{w} = \dot{u} = \dot{v} = 0$ ,

$$\begin{cases} -ax + yz + bw + \cos u = 0 \\ cy \tanh v - xz + k = 0 \\ xy - dz = 0 \\ xz - ew = 0 \\ gy = 0 \\ y^2 - v = 0 \end{cases} \tag{5}$$

that is, the equilibrium set of the system is obtained

$$E^* = \begin{cases} \text{None}, k \neq 0 \\ \left( \frac{\cos n}{a}, 0, 0, 0, 0, n \right), k = 0 \end{cases} \tag{6}$$

Next, when  $k = 0$ , the Jacobi matrix  $J_E$  of the system is shown below

$$J_E = \begin{bmatrix} -a & z & y & b & -\sin w & 0 \\ -z & c \tanh v & -x & 0 & 0 & -cy(\tanh^2 v - 1) \\ y & x & -d & 0 & 0 & 0 \\ z & 0 & x & -e & 0 & 0 \\ 0 & g & 0 & 0 & 0 & 0 \\ 0 & 2y & 0 & 0 & 0 & 0 \end{bmatrix} \tag{7}$$

The characteristic equation of the system is as follows

$$\lambda^6 + a_1 \lambda^5 + a_2 \lambda^4 + a_3 \lambda^3 + a_4 \lambda^2 + a_5 \lambda^1 + a_6 = 0 \tag{8}$$

where  $a_1 = 33.67, a_2 = 55.93, a_3 = -898.45, a_4 = -2371.36, a_5 = -335.28, a_6 = 6.73, \lambda_1 = -31.0102, \lambda_2 = 5.2430, \lambda_3 = -5.0048, \lambda_4 = -2.7456, \lambda_5 = -0.1691, \lambda_6 = 0.0178$ . According to the results obtained, it can be concluded that the system is erratic; therefore, it also provides theoretical support for the system to produce chaos.

### 3. Numerical Diagram of the Dynamical Behaviors

#### 3.1. Hidden Chaotic Attractor

According to Equation (6), when  $k \neq 0$ , there is no equilibrium point in the system, and the attractor of the chaotic system is called a hidden attractor. Here, when  $k = 7$  is set and the other parameters are adjusted, respectively, it is found that the system has various types of chaotic attractors, including a structurally symmetric type, multi-vortex type and single vortex type, as shown in Figure 2.

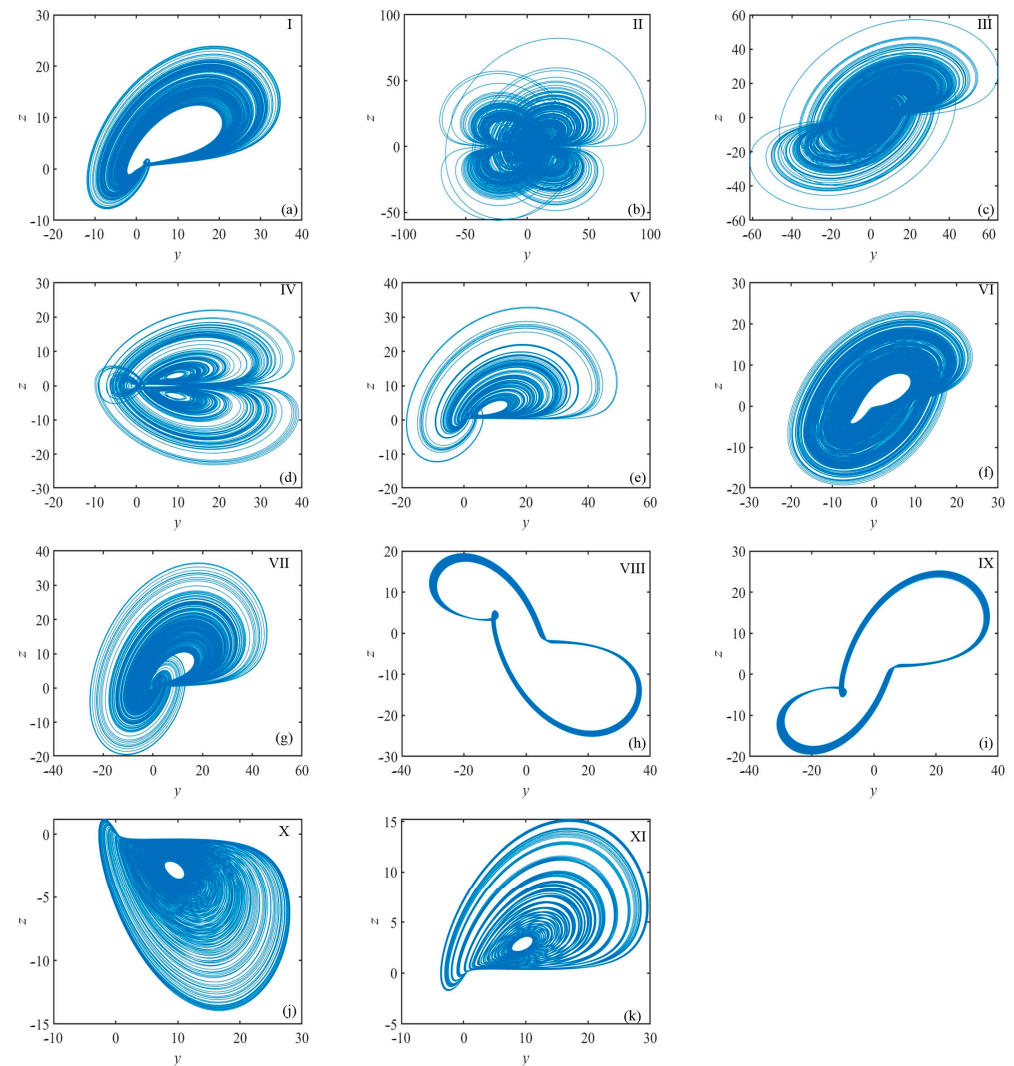


**Figure 2.** Hidden chaotic attractor of Type I-Type XI (Y-Z plane) under initial condition of (1, 1, 1, 1, 1), and  $b = 0.01, c = 5, k = 7, g = 0.05, l = 6$ , (a)  $a = 3, c = 7, d = 31$ ; (b)  $a = 5, c = 7, d = 31$ ; (c)  $a = 3, c = 12, d = 31$ ; (d)  $a = 3, c = 2.5, d = 31$ ; (e)  $a = 3, c = 6.7, d = 31$ ; (f)  $a = 3, c = 7, d = 11$ ; (g)  $a = 3.5, c = 7, d = 31$ ; (h)  $a = 8.24, c = 7, d = 31$ ; (i)  $a = 8.27, c = 7, d = 31$ ; (j)  $a = 3, c = 2, d = 31$ ; (k)  $a = 3, c = 2.0, 1d = 31$ .

#### 3.2. Analysis of Dynamic Characteristics

The LEs and bifurcation diagram is one of the classical methods to analyze nonlinear dynamic behavior. By fixing the other parameters and testing the data changes of the LEs and bifurcation diagram in different ranges of parameters  $a, c$  and  $k$ , respectively, the complex dynamic characteristics can be clearly understood.

When  $b = 0.01, c = 7, d = 31, k = 7, e = 5, g = 0.05, l = 6$ , choosing the initial conditions (1, 1, 1, 1, 1), and take the parameter  $a \in [2, 9]$ . By observing the LEs and bifurcation diagram in Figure 3, it can be seen that there are only two states; namely, the periodic state and the chaotic state. Under the change of parameter  $a$ , all state changes are summarized in

Table 1. The system exhibits strong sensitivity, as can be seen from  $a \in [8.26, 8.30]$ , where the attractor varies between Type VIII and Type IX.

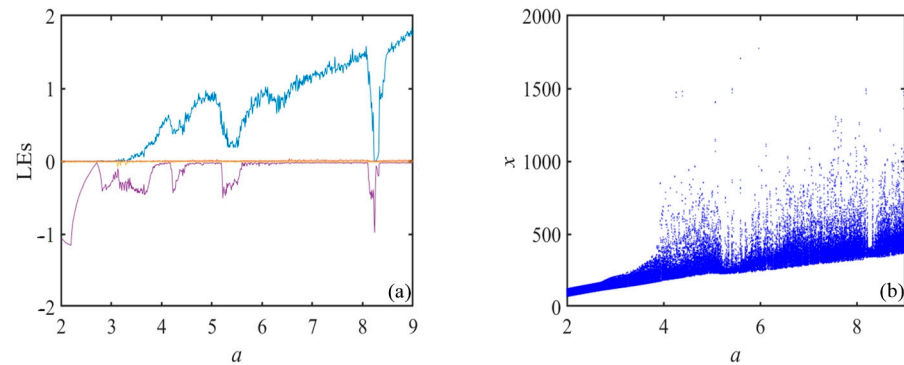


Figure 3. (a) Lyapunov exponent spectrum; (b) bifurcation diagram.

Table 1. Corresponding state and LEs with the initial conditions (1, 1, 1, 1, 1), the parameters  $b = 2$ ,  $c = 10$ ,  $d = 21$ ,  $k = 3$ ,  $e = 10$ ,  $g = 1.15$  and the different parameter  $a$ .

Range	LEs	State	Attractor Type	Range	LEs	State	Attractor Type
	0 - - - -	Divergence	None	8.26–8.27	+0 - - - -	Chaos	Type VIII
2–2.99	0 - - - -	Period	Period-1	8.28	+0 - - - -	Chaos	Type IX
3–3.44	+0 - - - -	Chaos	Type I	8.29	+0 - - - -	Chaos	Type VIII
3.45–3.94	+0 - - - -	Chaos	Type VII	8.30	+0 - - - -	Chaos	Type IX
3.95–8.22	+0 - - - -	Chaos	Type II	8.31–9	+0 - - - -	Chaos	Type II
8.23–8.24	+0 - - - -	Chaos	Type VIII	8.31–9	+0 - - - -	Chaos	Type II
8.25	+0 - - - -	Chaos	Type IX				

In order to explore the change of the chaotic attractor in the change of parameter  $c$ , choosing the initial condition is (1, 1, 1, 1, 1), and  $a = 3$ ,  $b = 0.01$ ,  $d = 31$ ,  $k = 7$ ,  $e = 5$ ,  $g = 0.05$ ,  $l = 6$ , the LEs and bifurcation diagram of the corresponding system when parameter  $c$  increases from 2 to 12, Under the change of parameter  $c$ , all state changes are summarized in Table 2, and shown in Figure 4.

Table 2. Corresponding state and LEs with the initial conditions (1, 1, 1, 1, 1), the parameters  $a = 10$ ,  $b = 2$ ,  $e = 5$ ,  $d = 21$ ,  $k = 3$ ,  $g = 1.15$  and the different parameter  $c$ .

Range	LEs	State	Attractor Type	Range	LEs	State	Attractor Type
	0 - - - -	Divergence	None	2.11–2.99	+0 - - - -	Chaos	Type IV
2–2.01	+0 - - - -	Chaos	Type X	3–6.59	0 - - - -	Period	Period-1
2.02–2.03	+0 - - - -	Chaos	Type IV	6.60–6.79	+0 - - - -	Weak chaos	Type V
2.04–2.05	+0 - - - -	Chaos	Type XI	6.79–10.61	+0 - - - -	Weak chaos	Type I
2.06–2.09	+0 - - - -	Chaos	Type IV	10.62–12	+0 - - - -	Chaos	Type III
2.1	+0 - - - -	Chaos	Type X				

At the interval  $2 \leq c \leq 2.1$ , it can be found that the chaotic attractor of the system is highly sensitive and transforms between Type X, Type XI and Type IV. Moreover, the chaotic attractor changes from single-scroll to multi-scroll and then reverts to single-scroll, and its multi-scroll has a high degree of symmetry, which is also a very interesting phenomenon.

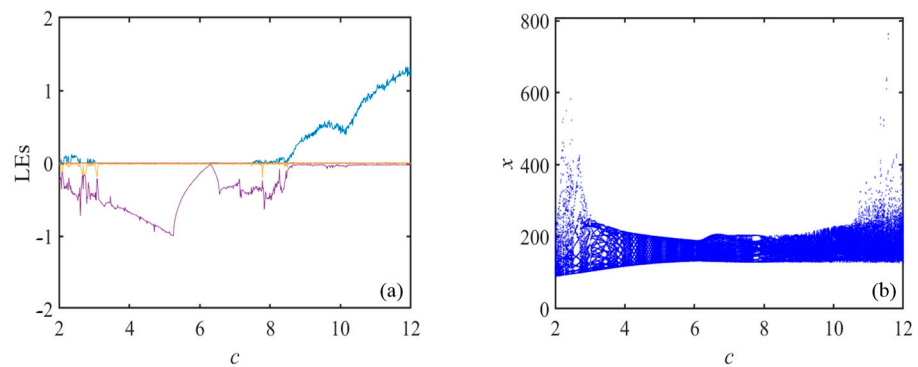


Figure 4. (a) Lyapunov exponent spectrum; (b) bifurcation diagram.

In order to further understand how parameter  $k$  affects the change of the chaotic attractor of the system, the initial condition is set as  $(1, 1, 1, 1, 1, 1)$ , letting parameter  $k \in [0, 8]$ , and  $a = 3, b = 0.01, c = 7, d = 31, e = 5, g = 0.05, l = 6$ . The LEs and its corresponding bifurcation diagram of variable parameter  $k$  is shown in Figure 5, and all state changes are summarized in Table 3.

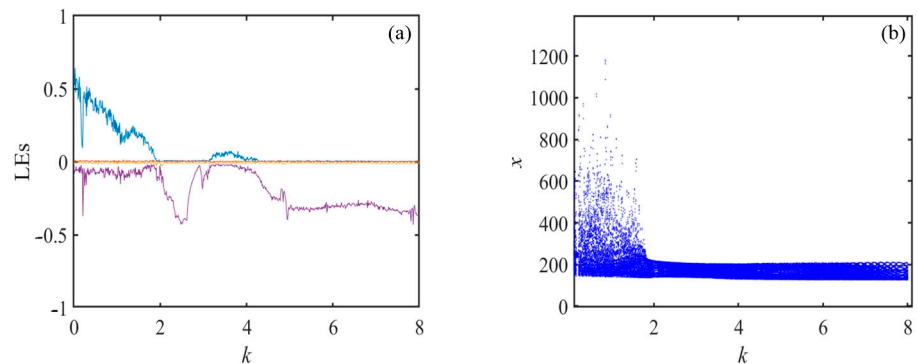


Figure 5. (a) Lyapunov exponent spectrum; (b) bifurcation diagram.

Table 3. Corresponding state and LEs with the initial conditions  $(1, 1, 1, 1, 1)$ , the parameters  $a = 10, b = 2, c = 10, d = 31, e = 10, g = 1.15$  and the different parameter  $k$ .

Range	LEs	State	Attractor Type	Range	LEs	State	Attractor Type
0–1.64	+0 ----	Chaos	Type II	2.02–3.03	+0 ----	Period	Period-2
1.65–1.88	+0 ----	Chaos	Type I	3.04–4.29	+0 ----	Chaos	Type I
1.89–2.01	+0 ----	Chaos	Type V	4.3–8	+0 ----	Period	Period-2

It can be observed from Figure 5 that when the parameter  $k \in [0, 1.64]$ , the maximum LEs is positive, and the bifurcation graph is in an obvious chaotic state. When parameter  $k \leq 2.02$ , the chaos attractors separate into different types, such as Type I, Type II and Type V. The specific dynamic characteristics under the different parameters of the system are recorded in Table 3.

From Tables 1–3, the types of some attractors are the same, but their chaotic states are different, which is closely related to the difference in the value of the maximum LEs. Sometimes the parameter change is not big, but its attractor state has great changes; this is also a situation that reflects the chaotic characteristics of the high sensitivity, it also provides theoretical support for the development of chaotic secure communication in the future.

### 3.3. Chaos Degradation

Chaos refers to the unpredictable and random-like motion of deterministic dynamical system due to its sensitivity to the initial value. Due to its unpredictability, as the time line lengthens, its possible chaotic state will become unstable, and it is possible to degenerate from the stable chaotic state to the periodic state, which is called chaos degradation. In the simulation of the system, when  $a = 3$ ,  $b = 0.01$ ,  $c = 2.05$ ,  $d = 31$ ,  $k = 7$ ,  $e = 5$ ,  $g = 0.05$ ,  $l = 6$ , and the initial condition is  $(1, 1, 1, 1, 1)$ . When  $t \in [0, 3450]$ , the system is in the chaos state and chaotic attractor as shown in Figure 6c, and when  $t > 3450$ s, the system quickly degenerates from the chaos state to the periodic state, as shown in Figure 6d.

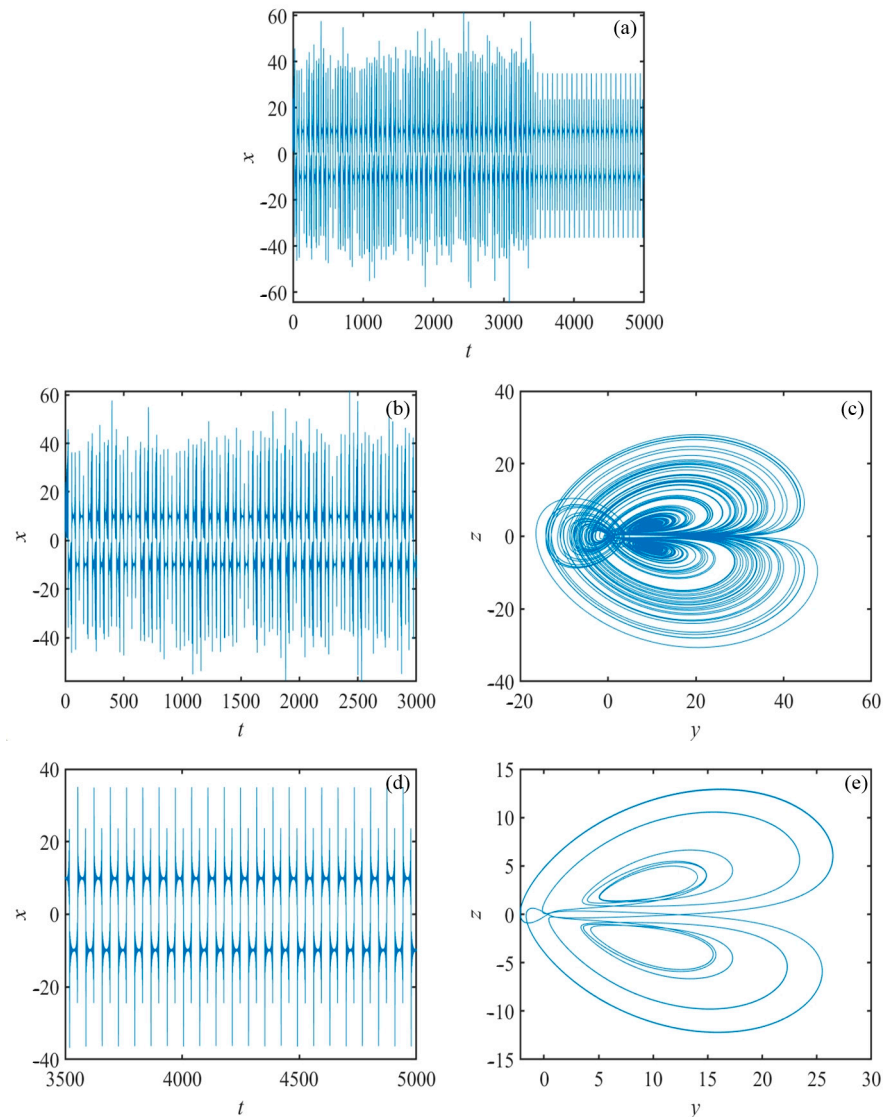


**Figure 6.** (a) time-domain waveform when  $t \in [0, 5000]$  (b) time-domain waveform when  $t \in [0, 3000]$  (c) chaotic attractor with  $t \in [0, 3000]$  (d) time-domain waveform when  $t \in [3000, 3500]$  (e) chaotic attractor with  $t \in [0, 3000]$ .

### 3.4. Coexisting-Attractors

Due to the high sensitivity of chaos to the initial value, it is found that when only the initial value of the chaotic system is changed, the chaotic attractor's position or shape changes are called coexisting-attractors. The high sensitivity of the initial value is one of the most important characteristics of chaotic systems, which means that the study of coexisting attractors has become one of the hot topics in nonlinear dynamics. As many different

attractors have been found in the simulation of the chaotic system, it is very meaningful to study the co-existence attractors of different attractors. When  $b = 0.01, e = 5, k = 7, g = 0.05, l = 6$ , the coexistence attractors in the Y-Z plane are shown in Figure 7, and their initial values are, respectively,  $(1, 1, 1, 1, 1, 1)$  and  $(1, 1, 1, 1, \pi, 1)$ .

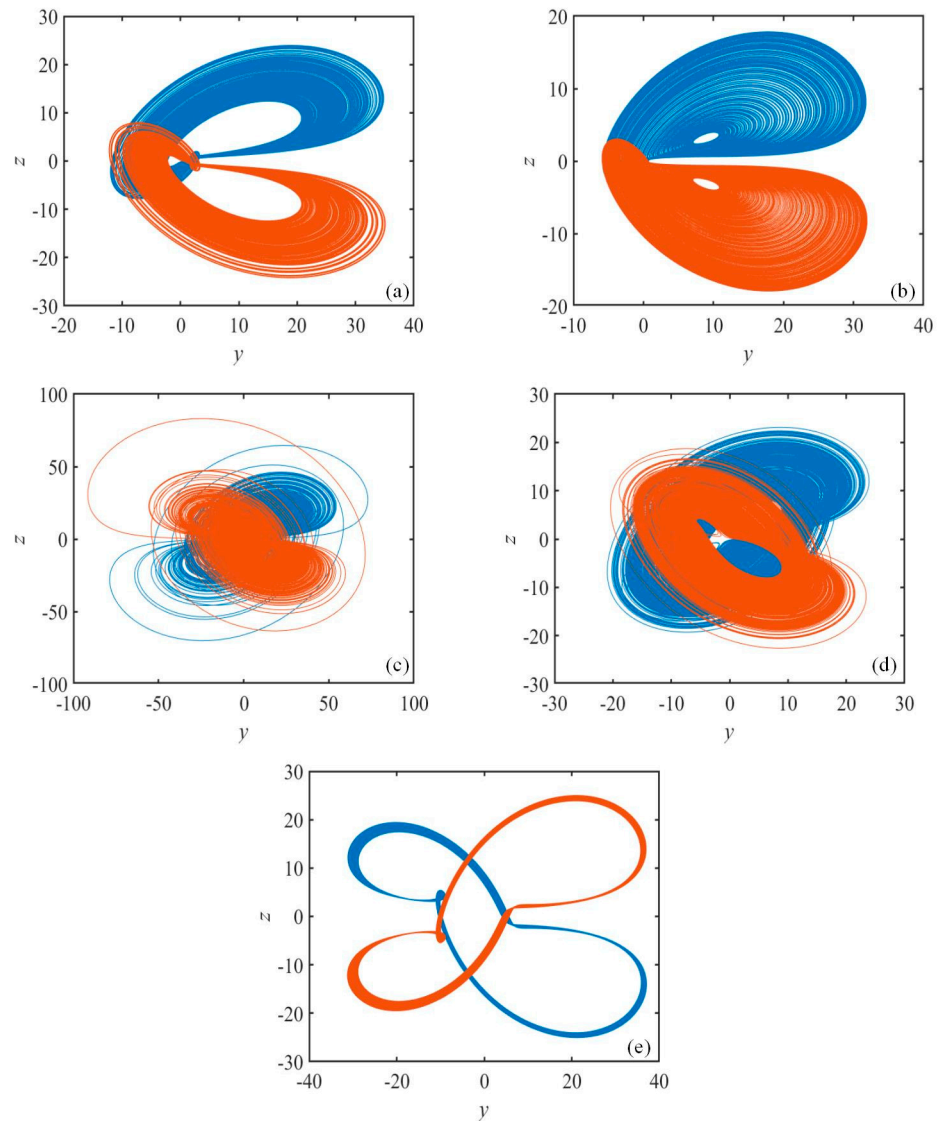


**Figure 7.** Y-Z plane with  $b = 0.01, e = 5, k = 7, g = 0.05, l = 6$ : (a)  $a = 3, c = 7, d = 31$ , when the initial conditions  $(1, 1, 1, 1, 1, 1)$  (blue) and  $(1, 1, 1, 1, 1, 1)$  (red); (b)  $a = 3, c = 2.4, d = 31$ , when the initial conditions  $(1, 1, 1, 1, 1, 1)$  (blue) and  $(1, 1, 1, 1, 1, 1)$  (red); (c)  $a = 3, c = 12, d = 31$ , when the initial conditions  $(1, 1, 1, 1, 1, 1)$  (blue) and  $(1, 1, 1, 1, 1, 1)$  (red); (d)  $a = 3, c = 7, d = 11$ , when the initial conditions  $(1, 1, 1, 1, 1, 1)$  (blue) and  $(1, 1, 1, 1, 1, 1)$  (red); (e)  $a = 8.24, c = 7, d = 31$ , when the initial conditions  $(1, 1, 1, 1, 1, 1)$  (blue) and  $(1, 1, 1, 1, 1, 1)$  (red).

### 3.5. Offset Boosting Scheme

The method of arbitrarily displacing chaotic attractors and their attractor pools without changing the system solution is called offset boosting. The specific method is to introduce a new variable and then control the system. As the system variable  $w$ , as an independent linear term, appears separately in the system equation, a new variable  $q$  is introduced to boost the variable  $w$ , thus achieving the effect of controlling the whole system. The improved system equation is shown below.

$$\begin{cases} \dot{x} = -ax + yz + b(w - q) + \cos u \\ \dot{y} = cy \tanh v - xz + k \\ \dot{z} = xy - dz \\ \dot{w} = xz - e(w - q) \\ \dot{u} = gy \\ \dot{v} = y^2 - v \end{cases} \quad (9)$$

Let the initial conditions be (1, 1, 1, 1, 1, 1), and the parameters  $a = 3, b = 0.01, c = 7, d = 31, k = 7, e = 5, g = 0.05, l = 6$ . Then, adjust the parameter  $q$  from 0 to 70, in sequence with step size 10. It can be observed from the 3-D diagram, shown in Figure 7, that the attractor moves straight along the direction of  $w$ . This means that the variable  $q$  can successfully control the movement of the attractor. Meanwhile, the bifurcation diagram in Figure 8b also showed a regular upward trend. Figure 8c,d shows the LES diagrams and bifurcation diagrams of parameter  $q \in [40, 50]$ , respectively. To facilitate observation, the smaller LEs are omitted. Hence, it clearly shows that the variables  $w$  increases as the offset  $q$  increases, while the LEs did not change. This means that the chaotic attractor does not undergo any change. According to the experimental results, it can be concluded that this method has a very significant effect on controlling the attractor displacement, and it has a very promising application prospect.

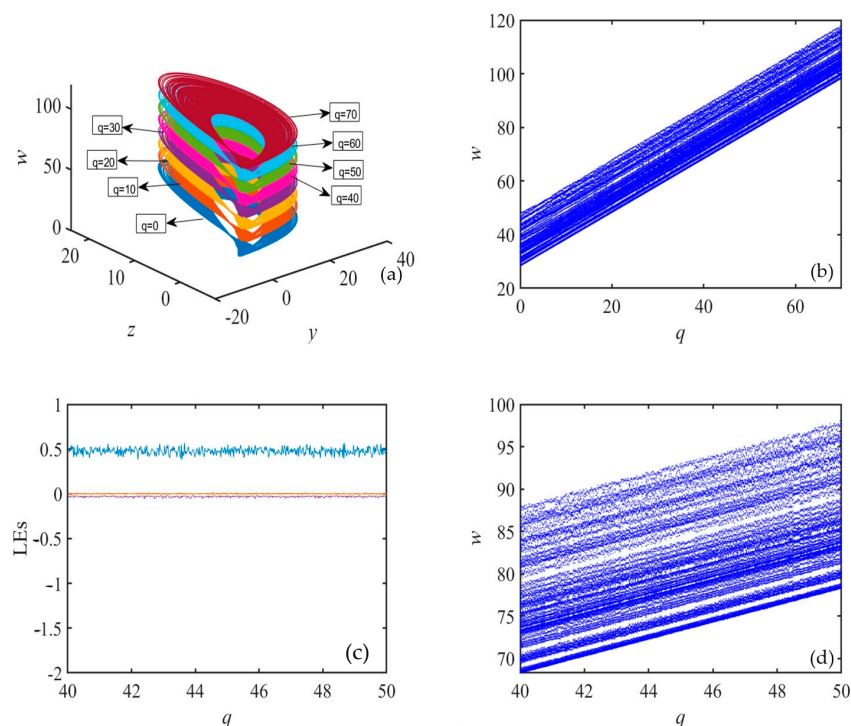


**Figure 8.** (a) Attractors with different offset  $q \in [0, 70]$ ; (b) bifurcation diagram with offset  $q \in [0, 70]$ . (c) Attractors with different offset  $q \in [40, 50]$ ; (d) bifurcation diagram with offset  $q \in [40, 50]$ .

### 3.6. Complexity Analysis

In general, the study of the complexity of chaotic systems is an important research index. By using a complexity algorithm to analyze the chaotic sequence and random sequence approximation, when the chaotic sequence is closer to the random sequence, it is proven that its complexity is higher. In order to study the influence of parameter changes on the system complexity, two different parameter combinations,  $a, d$  and  $a, k$ , are introduced. As shown in Figure 9a, when  $a$  and  $c$  increase continuously with the value, the color in the figure becomes increasingly darker, indicating higher complexity. This method also provides an effective basis for the parameter selection of the multivariable complex chaotic graph system.

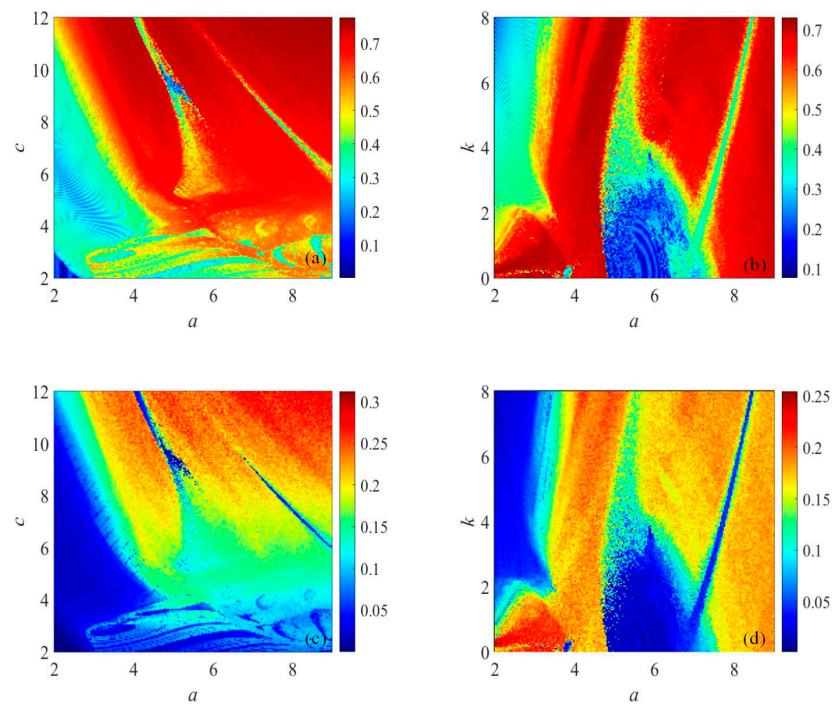


**Figure 9.** Initial conditions (1, 1, 1, 1, 1) with  $b = 0.01, d = 31, e = 5, g = 0.05, l = 6$ ; (a)  $k = 7$  with SE complexity Parameters of the  $a$  and  $d$ ; (b)  $c = 7$  with SE complexity Parameters of the  $a$  and  $e$ ; (c)  $k = 7$  with C0 complexity Parameters of the  $a$  and  $d$ ; (d)  $c = 7$  with C0 complexity Parameters of the  $a$  and  $e$ .

### 4. DSP Implementation

In order to verify the new memristor chaotic system, DSP is chosen to implement the system. The specific steps of the method for the DSP-controlled D/A converter on the sequence code is generated by the DSP corresponding simulation conversion, so that the output sequence is displayed on the oscillation range.

As the DSP platform can only deal with discrete data, it is necessary to deal with the continuous system first. The fourth order Runge-Kutta method is used to transform the data into a discrete chaotic sequence, and then the iterative relation is recorded into the DSP platform using C language. The operation process and experimental platform are shown in Figures 10 and 11.

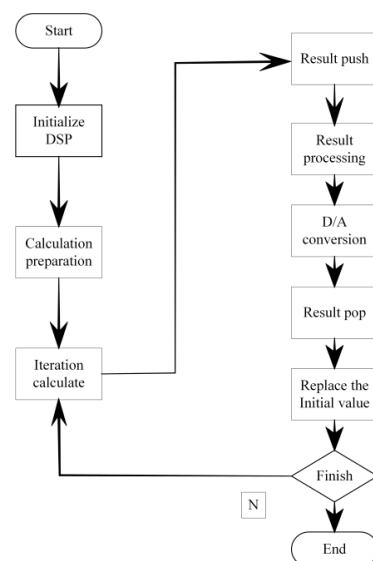


**Figure 10.** Programming flow of DSP implementation.

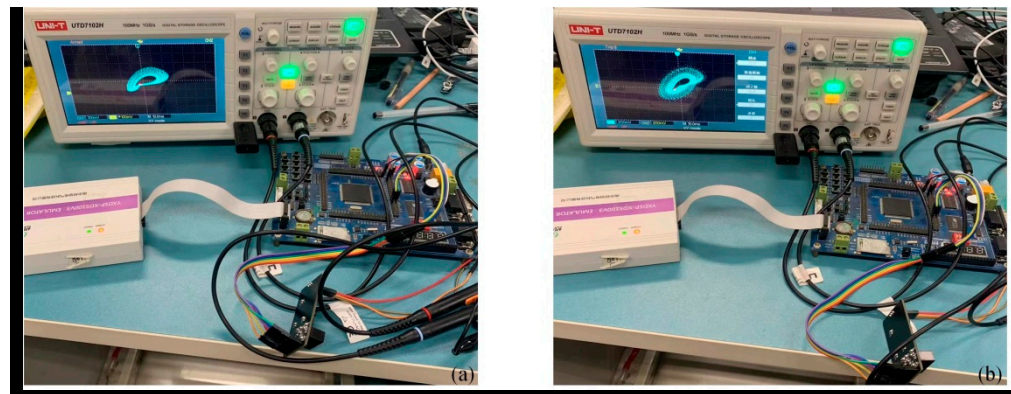


Figure 11. Experimental platform for DSP implementation; (a)  $a = 3, c = 7, d = 31$ ; (b)  $a = 3, c = 7, d = 11$ .

Let the parameter of the system  $b = 0.01, c = 5, k = 7, g = 0.05, l = 6$ . Let the parameter of the system initial condition  $(1, 1, 1, 1, 1, 1)$ , and change the other parameters to obtain the numerical simulation results, as shown in Figure 12:

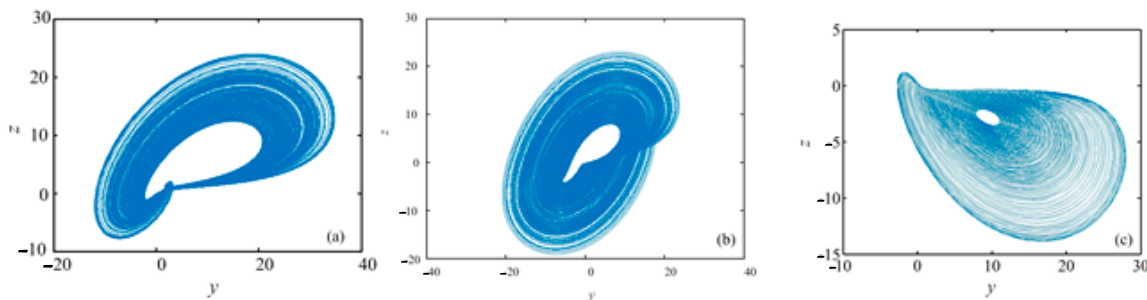


Figure 12. Phase diagram of chaotic attractor; (a)  $a = 3, c = 7, d = 31$ ; (b)  $a = 3, c = 7, d = 11$ ; (c)  $a = 3, c = 2, d = 31$ .

It can be observed in Figure 13 that the phase diagram realized on DSP is highly consistent with the phase diagram simulated, which proves the correctness of the digital circuit simulation of the system.

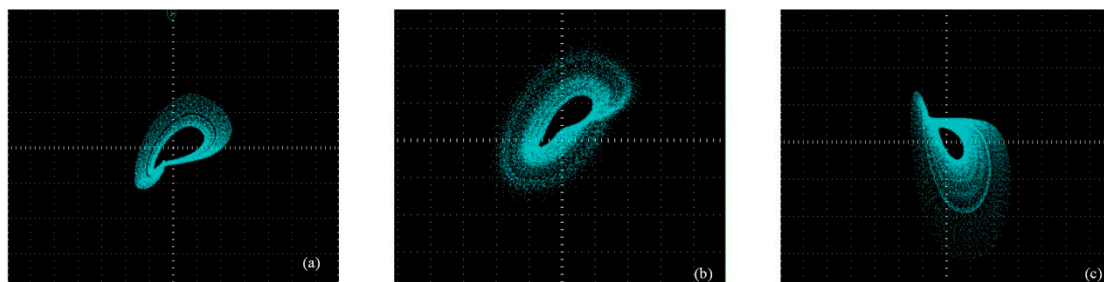


Figure 13. Chaotic attractor implemented on DSP platform; (a)  $a = 3, c = 7, d = 31$ ; (b)  $a = 3, c = 7, d = 11$ ; (c)  $a = 3, c = 2, d = 31$ .

### 5. Conclusions

In this paper, a new 6-D chaotic system is constructed by combining a memristor with a chaotic system, and its dynamical characteristics are studied numerically. By analyzing the phase diagram of the chaotic attractor, it is found that the system has many different types of hidden attractors, and the shape of the attractor changes with the change of parameters. At the same time, when the parameters change, the chaos will degenerate. In addition,

a new control variable  $q$  is introduced into the state variable  $w$  during the system bias boost. The state variable  $w$  varies linearly with the offset  $q$ , and its LES does not change significantly, which indicates that the  $w$  sequence can be flexibly changed by introducing control variables. Finally, the accuracy of the system simulation is verified on DSP. This paper provides a reference for the future research of the hidden chaotic attractor, bias boost and circuit implementation.

**Author Contributions:** Conceptualization and writing—original draft preparation, J.W.; Data curation, J.M.; Methodology, funding acquisition and writing—review and editing, Z.G. All authors have read and agreed to the published version of the manuscript.

**Funding:** This research was funded by Science and Technology Major Project of Shanxi Province (20181102023) and Beijing Social Science Foundation (Grant No. 20GLC052).

**Data Availability Statement:** All data is included in the paper.

**Conflicts of Interest:** The authors declare no conflict of interest.

## References

- Lin, H.; Wang, C.; Chen, C.; Sun, Y.; Zhou, C.; Xu, C.; Hong, Q. Neural Bursting and Synchronization Emulated by Neural Networks and Circuits. *IEEE Trans. Circuits Syst. I* **2021**, *68*, 3397–3410. [\[CrossRef\]](#)
- Lin, H.; Wang, C.; Yu, F.; Xu, C.; Hong, Q.; Yao, W.; Sun, Y. An extremely simple multiwing chaotic system: Dynamics analysis, encryption application, and hardware implementation. *IEEE Trans. Ind. Electron.* **2020**, *68*, 12708–12719. [\[CrossRef\]](#)
- Lin, H.; Wang, C.; Cui, L.; Sun, Y.; Xu, C.; Yu, F. Brain-Like Initial-Boosted Hyperchaos and Application in Biomedical Image Encryption. *IEEE Trans. Inform.* **2022**, *18*, 8839–8850. [\[CrossRef\]](#)
- Lin, H.; Wang, C.; Xu, C.; Zhang, X.; Lu, H.H.C. A Memristive Synapse Control Method to Generate Diversified Multi-Structure Chaotic Attractors. *IEEE Trans. Comput. Des. Integr. Circuits Syst.* **2022**. [\[CrossRef\]](#)
- Xu, C.; Wang, C.; Jiang, J.; Sun, J.; Lin, H. Memristive circuit implementation of context-dependent emotional learning network and its application in multi-task. *IEEE Trans. Comput. Aided Des. Integr. Circuits Syst.* **2021**, *41*, 3052–3065. [\[CrossRef\]](#)
- Deng, J.; Zhou, M.; Wang, C.; Wang, S.; Xu, C. Image segmentation encryption algorithm with chaotic sequence generation participated by cipher and multi-feedback loops. *Multimed. Tools Appl.* **2021**, *80*, 13821–13840. [\[CrossRef\]](#)
- Cheng, G.; Wang, C.; Xu, C. A novel hyper-chaotic image encryption scheme based on quantum genetic algorithm and compressive sensing. *Multimedia Tools Appl.* **2020**, *79*, 29243–29263. [\[CrossRef\]](#)
- Lin, H.; Wang, C.; Sun, Y.; Wang, T. Generating n-scroll chaotic attractors from a memristor-based magnetized hopfield neural network. *IEEE Trans. Circuits Syst. II* **2022**. [\[CrossRef\]](#)
- Zhou, Y.; Li, C.; Li, W.; Li, H.; Feng, W.; Qian, K. Image encryption algorithm with circle index table scrambling and partition diffusion. *Nonlinear Dyn.* **2021**, *103*, 2043–2061. [\[CrossRef\]](#)
- Li, C.; Zhou, Y.; Li, H.; Feng, W.; Du, J. Image encryption scheme with bit-level scrambling and multiplication diffusion. *Multimed. Tools Appl.* **2021**, *80*, 18479–18501. [\[CrossRef\]](#)
- Gao, X.; Mou, J.; Xiong, L.; Sha, Y.; Yan, H.; Cao, Y. A fast and efficient multiple images encryption based on single-channel encryption and chaotic system. *Nonlinear Dyn.* **2022**, *108*, 613–636. [\[CrossRef\]](#)
- Liu, X.; Mou, J.; Yan, H.; Bi, X. Memcapacitor-Coupled Chebyshev Hyperchaotic Map. *Int. J. Bifurc. Chaos* **2022**, *32*, 2250180. [\[CrossRef\]](#)
- Chu, Y.-M.; Bekiros, S.; Zambrano-Serrano, E.; Orozco-López, O.; Lahmiri, S.; Jahanshahi, H.; Aly, A.A. Artificial macro-economics: A chaotic discrete-time fractional-order laboratory model. *Chaos Solitons Fractals* **2021**, *145*, 110776. [\[CrossRef\]](#)
- Peng, Y.; He, S.; Sun, K. Chaos in the discrete memristor-based system with fractional-order difference. *Results Phys.* **2021**, *24*, 104106. [\[CrossRef\]](#)
- Li, X.; Mou, J.; Cao, Y.; Banerjee, S. An Optical Image Encryption Algorithm Based on a Fractional-Order Laser Hyperchaotic System. *Int. J. Bifurc. Chaos* **2022**, *32*, 2250035. [\[CrossRef\]](#)
- Gao, X.; Mou, J.; Banerjee, S.; Cao, Y.; Xiong, L.; Chen, X. An effective multiple-image encryption algorithm based on 3D cube and hyperchaotic map. *J. King Saud Univ. Comput. Inf. Sci.* **2022**, *34*, 1535–1551. [\[CrossRef\]](#)
- Han, X.; Mou, J.; Jahanshahi, H.; Cao, Y.; Bu, F. A new set of hyperchaotic maps based on modulation and coupling. *Eur. Phys. J. Plus* **2022**, *137*, 523. [\[CrossRef\]](#)
- Li, X.; Mou, J.; Banerjee, S.; Wang, Z.; Cao, Y. Design and DSP implementation of a fractional-order detuned laser hyperchaotic circuit with applications in image encryption. *Chaos Solitons Fractals* **2022**, *159*, 112133. [\[CrossRef\]](#)
- Sha, Y.; Bo, S.; Yang, C.; Mou, J.; Jahanshahi, H. A Chaotic Image Encryption Scheme Based on Genetic Central Dogma and KMP Method. *Int. J. Bifurc. Chaos* **2022**, *32*, 2250186. [\[CrossRef\]](#)
- Wang, C.; Zhou, L.; Wu, R. The Design and Realization of a Hyper-Chaotic Circuit Based on a Flux-Controlled Memristor with Linear Memductance. *J. Circuits, Syst. Comput.* **2018**, *27*, 1850038. [\[CrossRef\]](#)

21. Ren, L.; Mou, J.; Banerjee, S.; Zhang, Y. A hyperchaotic map with a new discrete memristor model: Design, dynamical analysis, implementation and application. *Chaos Solitons Fractals* **2023**, *167*, 113024. [[CrossRef](#)]
22. Li, C.; Li, H.; Xie, W.; Du, J. A S-type bistable locally active memristor model and its analog implementation in an oscillator circuit. *Nonlinear Dyn.* **2021**, *106*, 1041–1058. [[CrossRef](#)]
23. Wang, N.; Zhang, G.; Kuznetsov, N.; Bao, H. Hidden attractors and multistability in a modified Chua's circuit. *Commun. Nonlinear Sci. Numer. Simul.* **2021**, *92*, 105494. [[CrossRef](#)]
24. Cui, L.; Luo, W.-H.; Ou, Q.-L. Analysis and implementation of new fractional-order multi-scroll hidden attractors\*. *Chin. Phys. B* **2021**, *30*, 020501. [[CrossRef](#)]
25. Gong, L.-H.; Luo, H.-X.; Wu, R.-Q.; Zhou, N.-R. New 4D chaotic system with hidden attractors and self-excited attractors and its application in image encryption based on RNG. *Phys. A Stat. Mech. Appl.* **2022**, *591*, 126793. [[CrossRef](#)]
26. Wen, J.; Feng, Y.; Tao, X.; Cao, Y. Dynamical Analysis of a New Chaotic System: Hidden Attractor, Coexisting-Attractors, Offset Boosting, and DSP Realization. *IEEE Access* **2021**, *9*, 167920–167927. [[CrossRef](#)]
27. Itoh, M.; Chua, L.O. Memristor oscillators. *Int. J. Bifurc. Chaos* **2008**, *18*, 3183–3206. [[CrossRef](#)]
28. Hu, Z.; Li, Y.; Jia, L.; Yu, J. Chaotic Oscillator Based on Voltage-Controlled Memcapacitor. In Proceedings of the 2010 International Conference on Communications, Circuits and Systems (ICCCAS), Chengdu, China, 28–30 July 2010; pp. 824–827.
29. Yuan, F.; Wang, G.; Wang, X. Chaotic oscillator containing memcapacitor and meminductor and its dimensionality reduction analysis. *Chaos Interdiscip. J. Nonlinear Sci.* **2017**, *27*, 033103. [[CrossRef](#)]
30. Yuan, F.; Li, Y. A chaotic circuit constructed by a memristor, a memcapacitor and a meminductor. *Chaos Interdiscip. J. Nonlinear Sci.* **2019**, *29*, 101101. [[CrossRef](#)]
31. Yang, Y.; Huang, L.; Xiang, J.; Bao, H.; Li, H. Design of multi-wing 3D chaotic systems with only stable equilibria or no equilibrium point using rotation symmetry. *AEU Int. J. Electron. Commun.* **2021**, *135*, 153710. [[CrossRef](#)]
32. Sahoo, S.; Roy, B.K. Design of multi-wing chaotic systems with higher largest Lyapunov exponent. *Chaos Solitons Fractals* **2022**, *157*, 111926. [[CrossRef](#)]
33. Yang, Y.; Huang, L.; Xiang, J.; Bao, H.; Li, H. Generating multi-wing hidden attractors with only stable node-foci via non-autonomous approach. *Phys. Scr.* **2021**, *96*, 125220. [[CrossRef](#)]
34. Li, C.; Sprott, J.C.; Zhang, X.; Chai, L.; Liu, Z. Constructing conditional symmetry in symmetric chaotic systems. *Chaos Solitons Fractals* **2022**, *155*, 111723. [[CrossRef](#)]
35. Wang, R.; Li, C.; Kong, S.; Jiang, Y.; Lei, T. A 3D memristive chaotic system with conditional symmetry. *Chaos, Solitons Fractals* **2022**, *158*, 111992. [[CrossRef](#)]
36. Li, X.; Zheng, C.; Wang, X.; Cao, Y.; Xu, G. Symmetric coexisting attractors and extreme multistability in chaotic system. *Mod. Phys. Lett. B* **2021**, *35*, 2150458. [[CrossRef](#)]
37. Gu, S.; He, S.; Wang, H.; Du, B. Analysis of three types of initial offset-boosting behavior for a new fractional-order dynamical system. *Chaos Solitons Fractals* **2021**, *143*, 110613. [[CrossRef](#)]
38. Liang, Z.; Sun, K.; He, S. Design and dynamics of the multicavity hyperchaotic map based on offset boosting. *Eur. Phys. J. Plus* **2021**, *137*, 51. [[CrossRef](#)]
39. Zhang, X.; Li, C.; Dong, E.; Zhao, Y.; Liu, Z. A Conservative Memristive System with Amplitude Control and Offset Boosting. *Int. J. Bifurc. Chaos* **2022**, *32*, 2250057. [[CrossRef](#)]

**Disclaimer/Publisher's Note:** The statements, opinions and data contained in all publications are solely those of the individual author(s) and contributor(s) and not of MDPI and/or the editor(s). MDPI and/or the editor(s) disclaim responsibility for any injury to people or property resulting from any ideas, methods, instructions or products referred to in the content.